GLOBAL BIOGEOCHEMICAL CYCLES, VOL. 11, NO. 1, PAGES 111–124, MARCH 1997

Terrestrial carbon storage during the past 200 years: A Monte Carlo Analysis of CO_2 data from ice core and atmospheric measurements

Michele Bruno and Fortunat Joos

Physics Institute, University of Bern, Bern, Switzerland

Abstract. We have updated earlier deconvolution analyses using most recent high-precision ice core data for the last millennium [*Etheridge et al.*, 1996] and direct atmospheric CO_2 observations starting in 1958 [*Keeling and Whorf*, 1994]. We interpreted nonfossil emissions, that is, the difference between the increase in observed atmospheric plus modeled oceanic carbon inventory and fossil emissions, as biospheric carbon storage (release). We have assessed uncertainties in the CO_2 ice core data using a Monte Carlo approach and found a 2-σ uncertainty for the nonfossil emissions (20-year averages) of 0.2-0.4 GtC yr^{-1}. Overall uncertainties of the nonfossil emissions were estimated to be 0.5 GtC yr^{-1} before 1950 and $\sim$1 GtC yr^{-1} during the last decade. We found a large and rapid change of -0.8 GtC yr^{-1} in the nonfossil emissions (approximate net air-biota flux) between 1933 and 1943. Before 1933, the land biota acted as carbon source of order 0.5 GtC yr^{-1} in agreement with independent estimates of carbon emissions by land use changes [*Houghton*, 1993a]. After 1943, the land biota was a net sink of about 0.3 GtC yr^{-1}. This implies an average biospheric sink of 1.5 GtC yr^{-1} during the last 5 decades to compensate estimated carbon emissions by land use changes. We could not attribute this sink to a single mechanism. We found that the temporal evolution of the required biota sink is not compatible with conventional modeling of CO_2 fertilization. We estimated potential terrestrial carbon storage due to nitrogen fertilization to be 1 GtC yr^{-1} for 1960, that is, smaller than the required sink, and 1.5-3 GtC yr^{-1} for 1990. To assess the potential impact of climate variations, we deconvolved the preindustrial CO_2 concentrations which fluctuated around 280 ppm. We found a maximum nonfossil sink of 30 GtC within 50 years. Thus it seems not likely that the cumulative sink of 76 GtC which is required to balance land use emissions during 1935 to 1990 can be explained by climate variations only.

1. Introduction

High-precision ice core data [*Neftel et al.*, 1985; *Etheridge et al.*, 1996] and direct atmospheric observations [*Keeling and Whorf*, 1994] show that atmospheric CO_2 concentration has increased from its preindustrial level of about 280 Parts per million by volume (ppmv) to 360 ppmv today. As a consequence, the radiative properties of the atmosphere are changing significantly, inducing global climate change [*Houghton et al.*, 1994, 1996]. The growth in atmospheric carbon inventory between 1850 and 1990 (142 GtC) is less than half of the carbon emitted due to fossil fuel use and cement production (216 GtC) [*Marland et al.*, 1995; *Keeling*, 1994] and deforestation and other land use changes (98-128 GtC) [*Houghton*, 1993a]. The rest has been taken up by the ocean and the terrestrial biosphere.

Understanding the processes controlling this redistribution of anthropogenic CO_2 is a prerequisite to establish the relationship between future carbon emissions, atmospheric CO_2, and climate change. Carbon models of various complexity have been developed for this task to describe both oceanic uptake and carbon storage on land.

The global oceanic uptake of anthropogenic carbon at present climate conditions has been relatively well established by ocean modeling studies. Further, alternative reconstructions using as constraints observed oceanic nutrient and carbon distributions [e.g., *Chen*, 1993; *Gruber et. al.*, 1996], the observed distribution of atmospheric CO_2 [*Enting et al.*, 1995; *Heimann*

Paper number 96GB03611.
0886-6236/97/96GB-03611$12.00

and Keeling, 1989; *Tans et al.*, 1990; *Sarmiento and Sundquist*, 1992], measurements of surface ocean pCO_2 [*Takahashi et al.*, 1995; *Tans et al.*, 1990] , the distribution of ^{13}C in the climate system [*Quay et al.*, 1992; *Heimann and Maier-Reimer*, 1996; *Tans et al.*, 1993; *Ciais et al.*, 1995], or the temporal trend of the atmospheric O_2/N_2 ratio [*Keeling et al.*, 1996] support the ocean model results in general. The 2-σ uncertainty of the global ocean uptake during the 1980s is estimated to be 40% [*Schimel et al.*, 1994]. Modeled surface-to-deep ocean transport, that is, the rate limiting step for CO_2 uptake, can be independently validated by comparing modeled and observed penetration of time dependent tracers such as chlorofluorocarbons (CFCs), natural, and bomb-produced radiocarbon [*Revelle and Suess*, 1957; *Toggweiler et al.*, 1989; *Siegenthaler and Joos*, 1992]. On the other hand, it is difficult to validate biosphere models on a global scale by using biospheric observations with their large spatial and temporal variability. Thus the global uptake of anthropogenic carbon by the terrestrial system has been mainly deduced by difference to balance the global carbon budget given estimates of emissions, atmospheric, and oceanic carbon storage [*Siegenthaler and Oeschger*, 1987]. Moreover, biosphere models used to predict future anthropogenic CO_2 uptake are often validated or tuned in order to match the carbon budget, for example, for the last decade or for the historical period [*Enting et al.*, 1994; *Friedlingstein et al.*, 1995; *Sarmiento et al.*, 1995].

The classical method to calculate terrestrial carbon storage over time is by deconvolving the observed atmospheric CO_2 history [*Siegenthaler and Oeschger*, 1987]. Atmospheric CO_2 is prescribed in an ocean-atmosphere model, and the difference between the change in observed atmospheric $\frac{d}{dt}N_a$ plus modeled oceanic carbon inventory $\frac{d}{dt}N_{oc}$ and fossil emissions as deduced from trade statistics, p_f, is set equal to a so-called nonfossil emission term p_{nf}.

$$p_{nf}(t) = \frac{dN_a}{dt} + \frac{dN_{oc}}{dt} - p_f \qquad (1)$$

The term p_{nf} is usually interpreted as a net terrestrial carbon sink or source. This net flux between atmosphere and biosphere is the sum of opposing processes. Carbon is emitted due to deforestation and other land use changes [*Houghton*, 1993a]. Additional carbon is potentially sequestered on land due to elevated atmospheric CO_2 levels or enhanced nutrient input into the world's ecosystems, that is, fertilization [*Schimel et al.*, 1994]. It has been suggested [*Kauppi et al.*, 1992; *Dixon et al.*, 1994; *Kolchugina and Vinson*, 1993] based on forest inventories that much more carbon has been stored during forest regrowth in the northern hemisphere than assumed by *Houghton* [1993a]. This additional land use sink is neither included in the global figures of *Houghton* [1993a] nor accepted by *Houghton* [1993b]. The additional carbon stored on land due to fertilization, forest regrowth (as not already included in land use terms), and climatic effects can be estimated by subtracting the nonfossil emission term from the land use emissions.

The estimate of the net biospheric sink term is affected by various uncertainties. A fundamental assumption is that the natural carbon exchange between ocean and atmosphere is at balance on a decadal timescale. This assumption is roughly supported by the relatively small (<10 ppmv) preindustrial fluctuations of atmospheric CO_2 during the last millennium [*Etheridge et al.*, 1996; *Siegenthaler et al.*, 1988; *Barnola et al.*, 1995] and by comparison between simulated and observed decrease in $\delta^{13}C$ during industrial times [*Siegenthaler and Joos*, 1992]. Usually, the geochemical ocean models do not include interannual variability in the ocean-atmosphere exchange, for example, due to El Niño-Southern Oscillation (ENSO) events. Thus estimated nonfossil emissions should only be interpreted as biospheric fluxes on timescales larger than decades. Of minor importance are carbon fluxes in connection with volcanic activities and the weathering/sedimentation cycle which are assumed to be in balance as well [*Siegenthaler and Sarmiento*, 1993]. As it appears from equation (1), uncertainties in the estimated biospheric net fluxes are also due to uncertainties in fossil fuel emission estimates which are about 6-10% [*Marland and Rotty*, 1984; *Andres et al.*, 1996], in model estimates of oceanic uptake of anthropogenic CO_2, and in the atmospheric CO_2 observations.

Uncertainties in land use emissions translate into uncertainties in the estimated fertilization fluxes. Land use emissions which are derived by modeling the disturbance of terrestrial ecosystems by deforestation and other land use changes are highly uncertain. The magnitude of land use emissions has been revised substantially (order -40%) in the last 13 years [see, e.g., *King et. al.*, 1995].

The scope of this paper is to provide an update of earlier deconvolution simulations [*Siegenthaler and Oeschger*, 1987; *Sarmiento et al.*, 1992; *Siegenthaler and Joos*, 1992]. We use most recent high-precision CO_2 measurements obtained from firn and ice at a high accumulation site at Law Dome Antarctica [*Etheridge et al.*, 1996] combined with direct measurements of atmospheric CO_2 from Mauna Loa and south pole [*Keeling and Whorf*, 1994]. We estimate the uncertainty of the deduced terrestrial sink term due to uncertainties in atmospheric CO_2 data by using Monte Carlo statistics. Further, we compare results obtained by using the Law Dome data with those from the well-known Siple ice core CO_2 data [*Neftel et al.*, 1985]. To assess uncertainties in ocean uptake, we use four different ocean models: two box-type models, that is, the box-diffusion

model [*Oeschger et al.*, 1975] and the High-Latitude Exchange/Interior Diffusion-Advection (HILDA) model [*Siegenthaler and Joos*, 1992], a two-dimensional (2-D) model [*Stocker et al.*, 1994], and a three-dimensional (3-D) model [*Sarmiento et al.*, 1992]. The models are used in their mixed-layer pulse substitute representation [*Joos et al.*, 1996] to save computing power and to allow us to run the model several thousand times for the Monte Carlo simulations. We compare our estimates of the net terrestrial sink term with estimates of historical land use emissions and discuss implications for the global carbon cycle.

2. Input Data and Methodology

We calculated nonfossil emissions p_{nf} by solving the deconvolution equation (equation (1)). The fossil emissions have been prescribed according to *Marland et al.* [1995]. We do not explicitly prescribe emissions due to land use changes in our model runs. For further analysis, the land use term is subtracted from the nonfossil emission term after model simulations. This is of no importance as all source and sink terms are additive. Data from the three Antarctic cores DE08, DE08-2, and DSS [*Etheridge et al.*, 1996] and direct atmospheric measurements from Mauna Loa and South Pole [*Keeling and Whorf*, 1994] were used to reconstruct the history of atmospheric CO_2 from year 1006 to 1992 (Figure 1a). Monthly, seasonally adjusted Mauna Loa and South Pole data were averaged to yield a global mean record. Multiple ice core measurements at the same time are averaged. Then, the discrete ice core data and atmospheric mean values are combined and spline fitted [*Enting*, 1987] to obtain a continuous record. No corrections were applied to merge the two data sets. The continuous record is used as boundary conditions for the ocean model and to calculate the atmospheric growth rate (Figure 1a). For comparison, we also analyzed the Siple ice core CO_2 record [*Neftel et al.*, 1985] supplemented with measurements from the Antarctic cores D47 and D57 [*Barnola et al.*, 1995].

The spline fit method described by *Enting* [1987] acts as a low-pass filter. The cutoff period $T_{0.5}$, that is, the period at which the signal is attenuated by 50%, is a function of the approximated data spacing Δt, the weights given to individual points δ_i, and of a parameter λ:

$$T_{0.5} \cong 2\pi \left(\lambda \Delta t \delta_i^2\right)^{0.25} \qquad (2)$$

Data spacing Δt is 1 month for the atmospheric data and about 4 years for the ice core data. Note that the cutoff period depends only weakly on the exact data spacing. We selected the parameter (λ=25.66) and the relative weights between the ice core data (δ_{ice}=1) and the atmospheric data (δ_{atm}=0.069) to obtain approximate cutoff periods of 20 years for the ice core data and

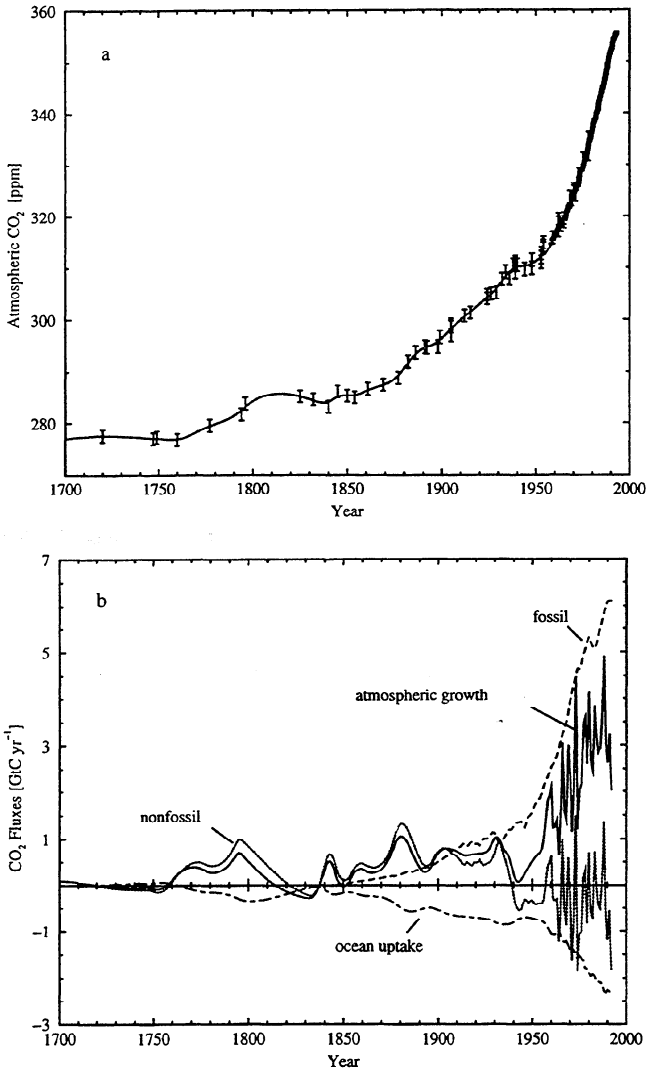

Figure 1. (a) Spline fit (solid curve) through the Law Dome ice core data [*Etheridge et al.*, 1996] and direct atmospheric measurements of CO_2 starting in 1958 [*Keeling and Whorf*, 1994]. Data points and 1-σ uncertainties of the ice core data ($\pm$1.2 ppmv) and of the deseasonalized monthly averaged CO_2 values from Mauna Loa and South Pole (0.1 ppmv) are indicated by error bars. The spline-fitting technique used is that of *Enting* [1987]. Approximate cutoff periods of 20 years for the ice core data and of about 2 years for the atmospheric data were applied; thus frequencies with shorter periods than the cutoff period were attenuated by 50% or more. (b) Results from a model deconvolution of the atmospheric CO_2 concentration history. The atmospheric growth rate (solid curve) is deduced from the spline fit of Figure 1a. Ocean uptake (long-dashed curve) is calculated with the HILDA model (version K(z) [*Siegenthaler and Joos*, 1992]) using the spline fit of Figure 1a as boundary condition. The fossil CO_2 production (dashed curve) is taken from *Marland et al.* [1995] and updated following personal communications. The nonfossil production rate (dotted curve) is the difference between the total increase in atmospheric and oceanic carbon inventory and the fossil production. It corresponds to the net contribution (emission minus uptake) of the terrestrial biota.

of 2 years for the period of direct atmospheric measurements. For the ice core data the 20 year cutoff period is motivated by the similar width of the age distribution of air in individual bubbles [*Etheridge et al.*, 1996]. Results are also presented for cutoff periods of 60 and 9 years, respectively.

The ocean carbon uptake was calculated with the HILDA model [*Siegenthaler and Joos*, 1992]. For comparison, we also calculated ocean uptake using the box-diffusion model [*Siegenthaler and Oeschger*, 1987], a 2-D model [*Stocker et al.*, 1994], and the Geophysical Fluid Dynamics Laboratory (GFDL)/Princeton 3-D model [*Sarmiento et al.*, 1992]. All models were run in their mixed-layer pulse response representation [*Joos et al.*, 1996]. Model runs were started at the year 1006 A.D. (beginning of the ice core record). Here we focus on results for the post-1800 period as data coverage is relatively sparse during preindustrial time and atmospheric CO_2 has varied relatively little before the onset of the industrial revolution.

We performed Monte Carlo simulations to assess the uncertainties in the nonfossil emission term as introduced by uncertainties in the ice core and atmospheric CO_2 measurements. 1-σ uncertainties are 1.2 ppm for individual ice core measurements and 0.1 ppm for the monthly atmospheric values. The Monte Carlo Analysis was done in the following way. In a first step a random data set was produced. For every point of the original data set a corresponding random data point was created using a random number generator [*Press et al.*, 1989, pp. 196-197, 202-203, functions RAN1 and GASDEV]. The Gaussian distribution of the generator for a specific data point corresponds to the value and the standard deviation of the original point. Next, the set of random data points was spline-fitted [*Enting*, 1987] and a deconvolution [*Siegenthaler and Oeschger*, 1987] using this spline fit to the random data as boundary condition in the HILDA model [*Joos et al.*, 1996; *Siegenthaler and Joos*, 1992] was performed. This procedure was repeated 2000 times for one Monte Carlo Analysis. At every point in time and for every model output variable, a 1-σ-confidence interval was obtained by requiring that 68% of the calculated values are within this interval. Such an analysis which corresponds to about 2 millions of model years required typically 9 hours of CPU time on a workstation (DEC 2100/500).

3. Results

Figure 1b shows the output of our standard deconvolution run in which a fit through the Law Dome ice core data and the atmospheric CO_2 measurements is used as boundary conditions in the HILDA model. The atmospheric growth rate as derived from this fit (Figure 1b, solid line) fluctuates approximately between 0 and 1 GtC yr^{-1} during the last century. Remarkable is its large breakdown at 1930. As noted by *Etheridge et al.* [1996], this anomaly may be linked to an unusually large ENSO event. The growth rate after 1960 exhibits large interannual variability. One should recall that a cutoff period of about 2 years was applied for the temporally better resolved atmospheric data as compared to 20 years for the ice core data. These short term variations are probably linked to ENSO events [*Keeling et al.*, 1989; *Siegenthaler*, 1990] and natural variations in both the atmosphere-ocean and atmosphere-land CO_2 exchange [*Francey et al.*, 1995; *Keeling et al.*, 1995]. The noticeable peak around 1959 may be an artifact caused by a small offset in ice core data and atmospheric measurements which start at 1958. The atmospheric CO_2 concentration (Figure 1a) and the modeled ocean uptake (Figure 1b) are relatively smooth. Modeled ocean uptake is only marginally reduced during period of low atmospheric growth as the uptake is rather a function of the atmospheric CO_2 concentration history and not of the instantaneous atmospheric growth rate. In other words, typical timescales of oceanic CO_2 uptake are longer than a few years. Natural interannual variability in air-sea exchange is not included in the ocean model. Fossil emissions are negligible before 1850 and increase about exponentially afterward.

The calculated nonfossil emissions follow approximately the atmospheric growth rate until 1940, while the difference between ocean uptake and fossil emissions are small. Most remarkable is that the nonfossil source of order +0.5 GtC yr^{-1} turned into an average sink of about -0.3 GtC yr^{-1} between 1933 and 1943. Total nonfossil emissions amount to 64 GtC during 1800-1940 (Table 1) and to 49 GtC during 1800-1992. The interannual fluctuations in p_{nf} after 1950 are linked to the mentioned interannual variability in the atmospheric growth rate and reflect perturbations in air-sea and air-biota exchange. We want to assess first uncertainties of p_{nf} before we further interpret these results.

3.1. Error Analysis

Uncertainties of the nonfossil production estimate p_{nf} are due to (1) uncertainties in the CO_2 data, (2) uncertainties in the modeled ocean uptake, and (3) uncertainties in the fossil emission estimate. Table 1 and Table 2 show nonfossil production rates as averaged over different time periods and associated uncertainties.

3.1.1. Uncertainties in the CO_2 data. We have performed 2000 runs using Monte Carlo statistics to investigate the link between uncertainties in the atmospheric CO_2 data and p_{nf}. We found for the Law Dome data a 1-σ uncertainty interval for the atmospheric growth rate (and thus for p_{nf}) of around ± 0.3 GtC yr^{-1} (Figure 2). Uncertainties in growth rate as deduced from the seasonally adjusted atmospheric CO_2 measurements are small (0.01 GtC yr^{-1}). 1-σ uncer-

Table 1. Nonfossil Emission Calculated by Deconvolving the Atmospheric CO_2 History as Reconstructed From the Law Dome Ice Core Data and Atmospheric Measurements at Mauna Loa and South Pole

Period	Average Nonfossil Emission, GtC yr^{-1}	Average Land Use Emission, GtC yr^{-1}	Difference Equal to Required Sink, GtC yr^{-1}
	1800-1990: 20- or 10-Year Intervals		
20-year intervals			
1800-1820	0.431 ± 0.202		
1820-1840	−0.073 ± 0.229		
1840-1860	0.365 ± 0.178		
1860-1880	0.621 ± 0.154	0.574	0.047
1880-1900	0.778 ± 0.135	0.673	0.105
1900-1920	0.607 ± 0.131	0.771	−0.164
1920-1940	0.513 ± 0.111	0.785	−0.272
1940-1960	−0.268 ± 0.058	0.888	−1.156
10-year intervals			
1960-1970	−0.233 ± 0.013	1.296	−1.529
1970-1980	−0.515 ± 0.011	1.308	−1.823
1980-1990	−0.094 ± 0.011	1.577	−1.671
	1800-1990: 50-Year intervals		
1800-1850	0.231 ± 0.063		
1850-1900	0.618 ± 0.053	0.599	0.019
1900-1950	0.368 ± 0.043	0.771	−0.403
1950-1990	−0.244 ± 0.030	1.304	−1.548
	Whole Period		
1800-1990	0.269 ± 0.015		

The Law Dome ice core data are from *Etheridge et al.* [1996], and atmopsheric measurements at Mauna Loa and south pole are from *Keeling and Whorf* [1994] (see Figure 1 and 2). Cutoff periods of 20 and 2 years were applied for the ice core and atmospheric data, respectively. The 1-σ confidence interval reflects uncertainties in the CO_2 data only as obtained by a Monte Carlo Analysis. Ocean uptake was calculated using the HILDA model [*Siegenthaler and Joos*, 1992]. The global carbon emissions due to deforestation and other land use changes are taken from *Houghton* [1993a]. The nonfossil emission is interpreted as net carbon uptake (or release) of the land biosphere. The difference between the nonfossil emission and carbon emission by land use changes is then the required sink (or source) to balance the global carbon cycle.

tainty intervals are between ±0.1 and ±0.2 GtC yr^{-1} for 20-year averages of p_{nf}, ±0.05 GtC yr^{-1} for 50-year averages, and ±0.015 GtC yr^{-1} for the period 1800-1990. Thus the uncertainty of the nonfossil emissions as induced by the Law Dome data is about 20% for 20-year averages but only 6% for the whole historical period (1800-1990). The error for this 190-year period due to CO_2 data is small because the total change in atmospheric CO_2 between 1800 and 1990 is well known and the ocean uptake is not very sensitive to changes in the CO_2 history. Estimated ocean uptake is 120 ± 1.4 GtC for 1800-1990. For 20-year averages, ocean uptake is uncertain by less than ± 0.1 GtC yr^{-1} due to uncertainties in the CO_2 data only.

The deconvolution of the Siple [*Neftel et al.*, 1985] ice core data (Figure 3) using the HILDA model has been performed in an earlier study [*Siegenthaler and Joos*, 1992]. Here we extended this analysis by applying our Monte Carlo method. To reconstruct the evolution of past atmospheric CO_2, we apply the same spline-fitting technique and the same cutoff period as above, namely 20 years for the ice core data and 2 years for the direct atmospheric measurements. We found similar results as for the Law Dome data. However, the 1-σ uncertainty band is about twice as wide for the Siple data (Figure 4). The improved precision of the *Etheridge et al.* [1996] CO_2 data is thus necessary to obtain accurate results for, for example, 20-year periods.

Table 2. 1-σ Confidence Intervals for Different Carbon Fluxes

	1-σ Uncertainties, GtC yr^{-1}					
	1	2	3	4	5	6
				1+2+3		4+5
Period	CO_2 Data	Fossil Fuel Data	Ocean Uptake	Nonfossil Emission	Land Use Data	Required Sink
20-year intervals						
1800-1820	±0.202	0	±0.057	±0.21		
1820-1840	±0.229	0	±0.018	±0.23		
1840-1860	±0.178	±0.004	±0.034	±0.18		
1860-1880	±0.154	±0.015	±0.058	±0.17	±0.18	±0.24
1880-1900	±0.135	±0.034	±0.106	±0.18	±0.20	±0.27
1900-1920	±0.131	±0.076	±0.130	±0.20	±0.24	±0.31
1920-1940	±0.111	±0.104	±0.159	±0.22	±0.25	±0.33
1940-1960	±0.058	±0.119	±0.155	±0.20	±0.28	±0.34
10-year intervals						
1960-1970	±0.013	±0.156	±0.231	±0.28	±0.41	±0.49
1970-1980	±0.011	±0.235	±0.317	±0.39	±0.41	±0.57
1980-1990	±0.011	±0.273	±0.417	±0.50	±0.49	±0.70

The uncertainty of (4) the nonfossil emission term is calculated by quadratic error addition of the uncertainties arising from uncertainties in (1) the CO_2 data, uncertainties in (2) fossil emissions, and (3) modeled ocean uptake. The uncertainty due to CO_2 data was obtained by a Monte Carlo Analysis. For the fossil emission a 1-σ uncertainty of 10% prior to 1950 and of 5% after 1950 was assumed [*Keeling*, 1973; *Marland and Rotty*, 1984]. 1-σ uncertainty of ocean uptake was estimated to be 20% [*Schimel et al.*, 1994]. 1-σ uncertainty of (5) land use emissions was estimated to be 31% which corresponds to a 2-σ error of 1 GtC yr^{-1} for the 1980-1990 period [*Schimel et al.*, 1994]. The overall uncertainty of (6) the required carbon sink was obtained by quadratic error additions of the uncertainties in (4) non-fossil emissions and (5) land use emissions.

We further investigated the influence of the cutoff period on calculated nonfossil emissions. Alternative to our standard simulation, we applied in the spline-fitting procedure larger cutoff periods of about 60 years for the Law Dome data and of 9 years for the atmospheric measurements. In Figure 5 the 1-σ uncertainty band is compared with the results of the standard simulation. The larger cutoff period leads to a smooth band but with the same general structure as found in the standard simulation. The interannual fluctuations during the last decades are suppressed by the stronger smoothing of the atmospheric data. Similarly, the shift in p_{nf} around 1940 appears less pronounced. The larger cutoff period results in a 1-σ error band of ±0.1 GtC yr^{-1} for the Law Dome data, that is, about 3 to 4 times smaller than for the standard case. This demonstrates that deduced nonfossil emissions as well as their uncertainties must be interpreted within the context of applied data smoothing. We recall that a filtering period of 20 years was chosen for the standard case in accordance with the age distribution of air bubbles in the Law Dome ice cores.

3.1.2. Uncertainty in modeled ocean uptake. Uncertainties in the modeled ocean uptake are directly linked to uncertainties in the nonfossil production term. The results of the Monte Carlo Analysis include the (small) uncertainties in ocean uptake which are due to uncertainties in the CO_2 history; however, uncertainties in surface-to-deep ocean mixing are not included. In Figure 6 the oceanic CO_2 uptake as calculated by four different ocean models are compared. The box-diffusion model (BD) shows the largest CO_2 uptake and the 3-D model shows the lowest. The HILDA model and the 2-D model give similar results and represent an average of the models considered here. A dip in the oceanic CO_2 uptake during the period from 1940 to 1960 is present in all four models. This feature is a consequence of the CO_2 plateau during the 1940s. The relative offsets between individual models are similar during most of the time. Differences between HILDA, 2-D, and 3-D models vanish only during periods of reduced atmospheric growth (e.g., around 1890 and 1940). We conclude that the choice of the model structure (box-type, 2-D, or 3-D) does not affect the temporal pattern of the deduced nonfossil production in a relevant way. However, the ocean model strongly affects the magnitude of p_{nf}. We find a cumulative nonfossil production between 1800 to 1990 of 44 GtC for the 3-D model, of 50 GtC, 51 GtC, and of 63 GtC for the 2-D model, for HILDA, and for the box-diffusion model, respectively. Cumulative ocean uptake for the four models are 113 (3-D), 119 (2-D), 120 (HILDA), and 132 GtC (BD). It may be noted that the four models presented here do not span the uncertainty currently associated with the

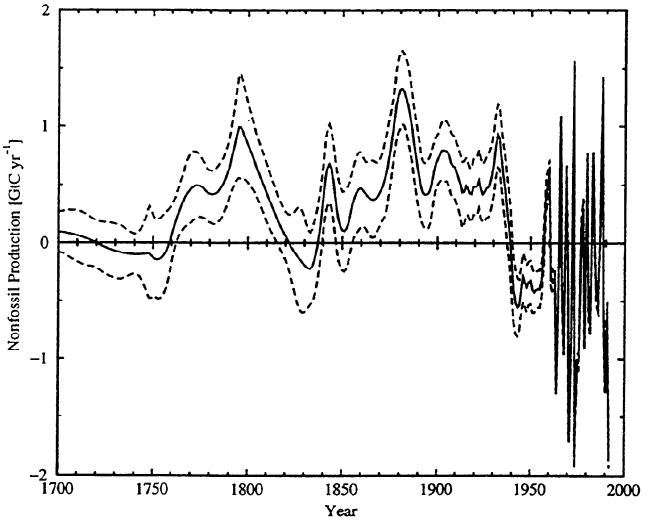

Figure 2. 1-σconfidence interval (dashed curve) of the nonfossil production rate reflecting uncertainties in the CO_2 data only as obtained by a Monte Carlo Analysis for the Law Dome ice core data and the atmospheric measurements (1958 and following). The best estimate (solid curve) corresponds to the dotted curve in Figure 1b. The Monte Carlo Analysis includes 2000 runs. For each run all measurements were varied within their uncertainties using a random number generator. Then a spline fit through the new randomly produced record is calculated, and a deconvolution is performed using the spline fit as model input. Approximate cutoff periods of 20 years for the ice core data and of 2 years for the atmospheric data were applied for the spline filtering.

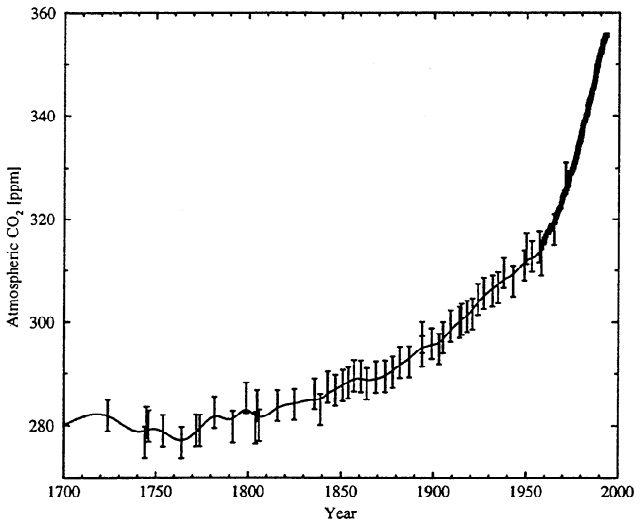

Figure 3. As for Figure 1a, but ice core data are those from Siple [*Neftel et al.*, 1985] plus measurements from the Antarctic cores D47 and D57 [*Barnola et al.*, 1995]. Approximate cutoff periods of 20 years were applied for the ice core data and of 2 years for the atmospheric measurements. These ice core data have a typical 1-σ uncertainty of ± 3 ppmv.

oceanic uptake of anthropogenic CO_2, that is 2.0 ± 0.6 GtC yr^{-1} (30%) [*Siegenthaler and Sarmiento*, 1993] to 2.0 ± 0.8 GtC yr^{-1} (40%) [*Schimel et al.*, 1994] for the 1980-1989 decade. All ocean models considered here do not include any natural variations of the ocean carbon cycle.

3.1.3. Uncertainties in fossil emissions. Finally, uncertainties in fossil emissions translate into uncertainties of the deduced nonfossil emissions. The accuracy of the fossil fuel data depends on the completeness of the compiled statistics on fossil fuel trade and energy consumption. *Marland and Rotty* [1984] and *Andres et al.* [1996] assume an uncertainty of 6-10% on a 90% confidence level for the postwar period. Uncertainties are probably much larger and are estimated to be around 20% (90-95% confidence level) for the pre-1950 period [*Keeling*, 1973]. Although, results of a recent compilation by *Andres et al.* [1996] agree within 5% with data published by *Keeling* [1973] for the years 1860 to 1953. *Keeling* [1973] provides results of five different studies which yielded cumulative emissions in the range 13.5-20.3 GtC for the years 1940-1949. Keeling's own estimate is the lower limit.

3.1.4. Overall uncertainty. We estimated total uncertainty (2-σ) associated with a 20-year average of the estimated nonfossil emission to be roughly equal or smaller than ± 0.5 GtC yr^{-1} for the period prior to 1950 (Table 2). This estimate was obtained by quadratic error addition, thereby assuming that uncertainties arising from the ice core measurements and uncertainties in ocean uptake and fossil emissions are independent. Uncertainties of 40% for estimated ocean uptake and of

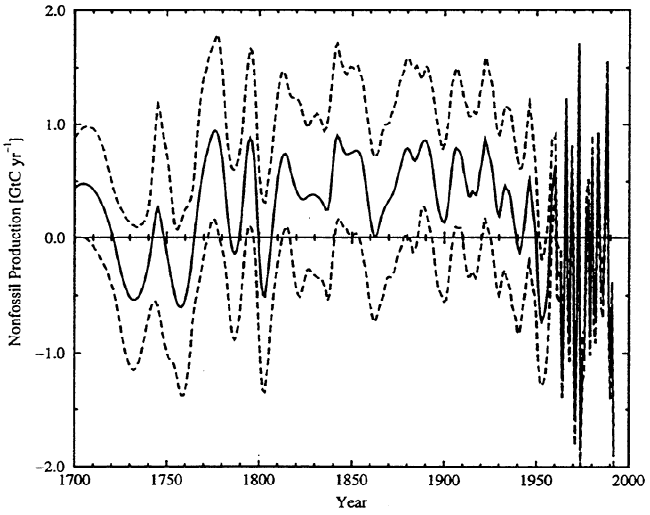

Figure 4. As for Figure 2, but ice core data are those from Siple and D47/D57 as shown in Figure 3. The 1-σ confidence interval (dashed curve) is about twice as large using the Siple data as compared to the Law Dome ice core data.

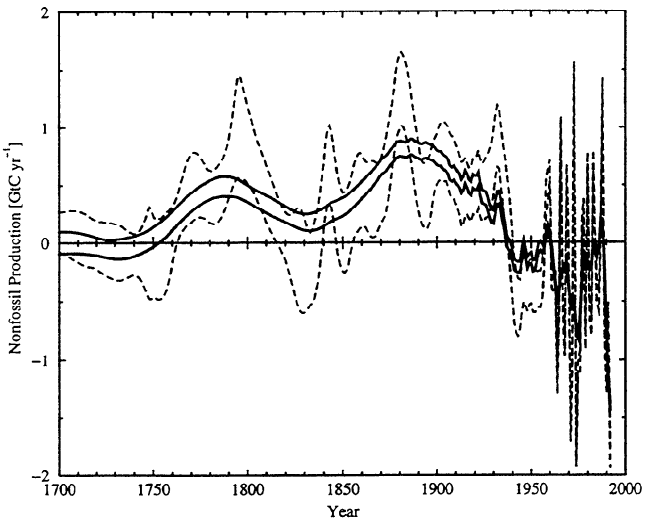

Figure 5. As for Figure 2, but the 1-σ confidence intervals of the nonfossil emissions for cutoff periods of 60 years for the ice core data and of 9 years for the atmospheric data (solid curve) are compared to the standard case (dashed curves, cutoff periods: 20 years and 2 years). The confidence interval reflects uncertainties in the Law Dome ice core and atmospheric data only.

20% for the fossil emissions were assumed. Individual 2-σ uncertainties range between 0.12 and 0.46 GtC yr^{-1} for uncertainties associated with the ice core data, between 0 and 0.31 GtC yr^{-1} for the ocean uptake (40%) and between 0 and 0.2.4 GtC yr^{-1} (20%) for the fossil fuel data. For the last decades, only uncertainties associated with modeled ocean uptake and fossil emission estimate contribute significantly to the overall uncertainty. This is of order ± 1 GtC yr^{-1} for the 1980s.

3.2. Discussion

We interpreted the short-term variations (after 1960) in the atmospheric growth rate and in the nonfossil emission term as natural fluctuations of both air-sea and air-biota exchange. These interannual variations of several GtC yr^{-1} can only be reconstructed from the direct atmospheric measurements as the process of bubble close off during ice formation acts as a low-pass filter. Analyses of recent CO_2 and $\delta^{13}C$ measurements suggest that these interannual variations are due to both atmosphere-ocean and atmosphere-land CO_2 exchange [*Francey et al.*, 1995; *Keeling et al.*, 1995]. Similarly, field studies [*Inoue and Sugimura*, 1992,1995; *Wong et al.*, 1995] show a large year-to-year variability in ocean surface pCO_2 and in deduced air-sea fluxes. *Winguth et al.* [1994] find in their general ocean circulation model a temporary oceanic carbon uptake of 0.6 GtC and a concurrent terrestrial carbon release of about 2 GtC during the ENSO year 1983. Several other studies suggested also an enhanced CO_2 uptake by the oceans during ENSO events [*Volk*, 1989; *Siegenthaler*, 1990; *Keeling et al.*, 1989].

We interpreted the decadal trend of the nonfossil term as net biospheric source or sink. This interpretation is in general supported by a preliminary analysis (double deconvolution [*Keeling et al.*, 1989]) of unpublished $\delta^{13}C$ measurements at the Law Dome site (R. Francey and M. Leuenberger, personal communication, 1994).

The most pronounced feature in the nonfossil emission history is the abrupt shift between 1933 and 1943 (Figures 2 and 7). After 1940 and the century before 1930, there is no clear trend visible in p_{nf} (Figure 7). On a 20-year average basis the magnitude of the nonfossil emission changed by about 0.8 GtC yr^{-1} from a level of +0.5 GtC yr^{-1} to -0.3 GtC yr^{-1}. This is of about equal size as the estimated ocean uptake and about two thirds of the fossil emissions at this time. The peak-to-peak difference between 1933 and 1943 is 1.5 GtC yr^{-1}. Thus the shift is clearly larger than associated uncertainties. However, around 1940 ocean uptake was probably enhanced due to a strong El Niño (1939-1942) and the transition of the net-biota sink might be less sharp than it appears in Figure 2 or 7.

Various earlier deconvolution analyses [*Sarmiento et al.*, 1992; *Siegenthaler and Oeschger*, 1987; *Siegenthaler and Joos*, 1992] yield not such an abrupt change in the nonfossil emission rate. The difference arises because the atmospheric input data are smoothed more extensively in these previous studies as the uncertain-

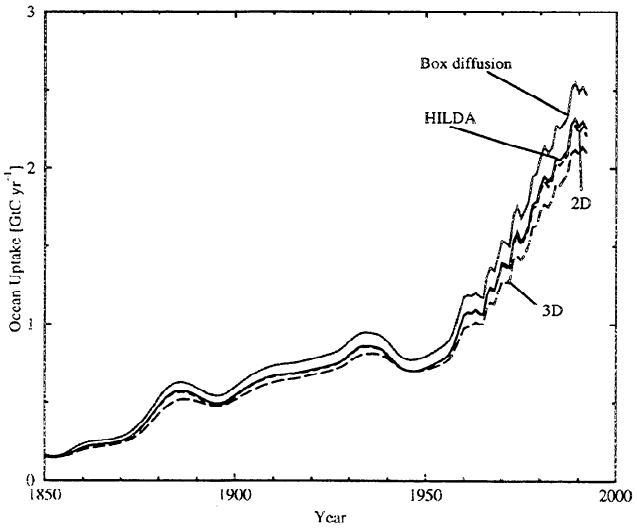

Figure 6. Ocean uptake of anthropogenic CO_2 as calculated with the box diffusion (dotted curve [*Oeschger et al.*, 1975]), the HILDA (solid curve [*Siegenthaler and Joos*, 1992]), a dynamical 2-D model (dashed curve [*Stocker et al.*, 1994]), and the Princeton/Geophysical Fluid Dynamics Laboratory(GFDL) ocean general circulation model [*Sarmiento et al.*, 1992]. All results are obtained by using the mixed-layer pulse response technique [*Joos et al.*, 1996].

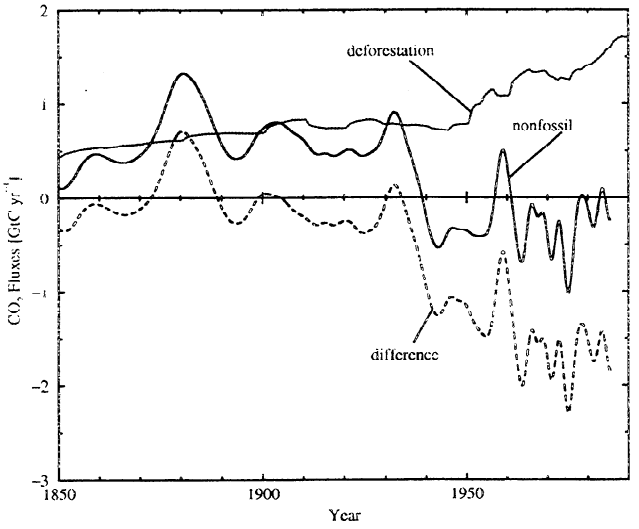

Figure 7. The nonfossil emissions (solid curve), that is, the net carbon release/uptake of the land biota, are compared to an independent estimate of carbon emissions due to deforestation and other land use changes (dotted curve [*Houghton*, 1993a]). The nonfossil emissions are as in Figure 1a (dotted curve) but filtered with a low-pass filter (cutoff period: 5 years) to remove interannual variability. The peak at 1959 is probably an artifact arising by linking the atmospheric and ice core data. The difference between net biota uptake and land use emissions (dashed curve) corresponds to a biotic sink (or source) required to balance the anthropogenic carbon budget.

ties of the Siple data are larger than those of the Law Dome data. We found a similar shift for the Siple data when applying the same filtering technique as used for the Law Dome data (Figure 4). *Sarmiento et al.* [1995] linearly interpolated individual Siple ice core measurements and deseasonalized monthly averaged atmospheric measurements for a deconvolution analysis. They found a similar terrestrial net uptake until about 1940 and then a brief transition period between 1940 and 1950 and a roughly constant terrestrial uptake afterward in agreement with our results. However, large variability due to their data treatment obscure the real trend before the onset of the direct atmospheric measurements.

In Figure 7 and Table 1 our nonfossil emission estimates are compared with independent estimates of global carbon emissions due to deforestation and other land use changes [*Houghton*, 1993a]. To ease interpretation, the nonfossil emission output has been filtered to remove the interannual variations (low-pass filter with a cutoff period of 5 years). The land use data indicate a biospheric source of slightly more than 0.5 GtC yr^{-1} between 1850 and 1950, afterward land use emissions increase to reach about 1.7 GtC yr^{-1} in 1990. Emission data from changing land use have large uncertainties (Table 2). Houghton estimated a cumulative emission from 1850-1990 of 98-128 GtC [*Houghton*, 1993a] and of 122 ± 40 GtC (as cited by *Schimel et al.* [1994]). For the last decade, land use emissions are estimated to be 1.6 ± 1.0 GtC yr^{-1}. Prior to 1930, our estimated nonfossil emissions agree within their uncertainty with the land use data. This suggests that no additional sink or source is required to balance the carbon cycle. After 1940, the difference between p_{nf} and land use data is substantial. If the land use data are accepted, an additional average sink of 1.5 GtC yr^{-1} is needed for the 1950-1990 period to balance the carbon budget. The cumulative difference between land use data and p_{nf} increases from a value close to zero in 1935 to about 76 GtC in 1990.

How can the difference between the land use data and the deduced net biospheric sink be explained? Several postulated mechanisms of biospheric carbon uptake can be found in the literature. These include (1) plant fertilization due to the increase in atmospheric CO_2, (2) fertilization by enhanced nitrogen deposition, and (3) climate induced variations [*Schimel*, 1995]. In the following paragraphs, we will discuss these mechanisms based on literature. We will present fertilization fluxes calculated with a 4-box biosphere model and compare

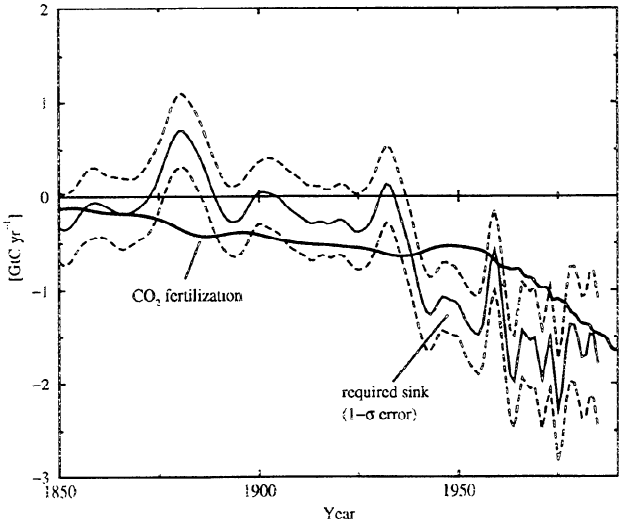

Figure 8. The temporal pattern of modeled carbon storage due to CO_2 fertilization (thick solid curve) does not match the land biosphere sink (solid curve) in Figure 7 which is required to balance the land use emission estimate of *Houghton* [1993a]. The dashed curves show the 1-σ uncertainty band of the required sink as given in Table 2, column 7. CO_2 fertilization is modeled using a 4-box model [*Siegenthaler and Oeschger*, 1987; *Joos et al.*, 1996] and a logarithmic dependency of primary productivity on atmospheric CO_2 ($npp = \beta \ln(CO_2/280ppm)$) . The coupling parameter β (=0.38) is tuned in order to balance an average land use emission of 1.6 GtC yr^{-1} during the last decade.

the results with the additionally required sink, calculate upper bounds for historical carbon storage due to nitrogen fertilization, and finally investigate potential climatic effects on carbon storage by deconvolving the preindustrial CO_2 history.

3.2.1. CO_2 fertilization. CO_2 fertilization is widely accepted to play a role in the current terrestrial carbon budget [*Schimel et al.*, 1994]. A stimulation of leaf photosynthesis and plant growth by elevated CO_2 levels is found in many pot studies. However, it is much less clear whether elevated CO_2 levels also result in an increased carbon storage on an ecosystem level [*Körner*, 1993; *Bazzaz*, 1990]. Field studies and studies in artificial ecosystems show decreasing, small or statistically insignificant responses [*D'Arrigo and Jacoby*, 1993; *Körner and Arnone III*, 1992; *Norby et al.*, 1992; *Oechel et al.*, 1993]. A recent modeling study of *King et al.* [1995] does also suggest that CO_2 fertilization can only explain a small portion (~20%) of the difference between land use and nonfossil emissions, whereas other model studies suggest a significant CO_2 fertilization [e.g. *Esser*, 1987; *Friedlingstein et. al.*, 1995; *Ludeke et. al.*, 1995]. We have estimated carbon uptake by CO_2 fertilization using a 4-box biosphere [*Siegenthaler and Oeschger*, 1987] in combination with a logarithmic β factor relationship between additional photosynthesis and atmospheric CO_2 (β=0.38 [*Joos et al.*, 1996]). A Michaelis-Menten type, hyperbolic function has been suggested as more appropriate to describe the relationship between atmospheric CO_2 and stimulated photosynthesis . However, the difference between the two formulations is of no importance in the present context [*Friedlingstein et al.*, 1995]. The β factor has been tuned in order to balance an average land use flux of 1.6 GtC yr^{-1} during the 1980s. This simple biosphere model has also been used for the reference Intergovernmental Panel on Climate Change (IPCC) scenario calculations linking anthropogenic emissions and atmospheric CO_2 [*Schimel et al.*, 1996]. It shows a similar temporal pattern in carbon storage as more complex models [*Esser*, 1987; *Friedlingstein et al.*, 1995]. In Figure 8 modeled carbon storage by CO_2 fertilization and our deduced biospheric carbon sink are compared. The temporal trend in the modeled fertilization flux is substantially different from the trend in our deduced sink, that is, the difference between land use and nonfossil emissions. For example, a sink term larger than 1 GtC yr^{-1} is necessary as early as 1940 to balance the land use flux, whereas the modeled fertilization flux exceeds a value of 1 GtC yr^{-1} about 30 years later. The results suggest that conventionally modeled CO_2 fertilization alone cannot explain the deduced biospheric sink. However, it was shown that the mismatch between required sink and modeled fertilization can be overcome, if a logistic growth function is applied instead of a logarithmic dependency of net primary production (NPP) on atmospheric CO_2 (e.g. [*Moore III and Braswell*, 1994; *Sarmiento et al.*, 1995]).

3.2.2. Nitrogen fertilization. We next address the question whether nitrogen fertilization has the potential to support a carbon storage of 1.5 GtC yr^{-1} during the last decades. Presently, about 140 TgN yr^{-1} are fixed by anthropogenic activities [*Galloway et al.*, 1995; *Kinzig and Socolow*, 1994] such as fertilizer production (80 TgN yr^{-1}), planting of leguminous crops (40 TgN yr^{-1}), and fossil fuel combustion (20 TgN yr^{-1}). Some of this nitrogen might stimulate additional plant growth as many ecosystems are nitrogen limited [*McGuire et al.*, 1992]. *Peterson and Melillo* [1985] suggest an additional carbon storage of the order 0-0.2 GtC yr^{-1} and *Schindler and Bayley* [1993] estimated that there is a possible carbon sink of 1-2.3 GtC yr^{-1} based on nitrogen deposition due to fossil fuel use alone. *Townsend et al.* [1996] using a spatially resolved terrestrial biosphere model and maps of fossil fuel nitrogen deposition find that fertilization due to fossil fuel nitrogen only accounts for 0.44-0.74 GtC yr^{-1} carbon storage in 1990 and for a cumulative sink of 18-27 GtC for the 1845-1990 period. They further find that fertilization is most important north of 30°N. *Schimel et al.* [1994] attributed a sink of about 0.5± 0.5 GtC yr^{-1} to northern hemisphere forest regrowth for the last decade based on forest inventories [*Kauppi et al.*, 1992; *Dixon et al.*, 1994; *Kolchugina and Vinson*, 1993]. This sink might be due to nitrogen fertilization. Recall that such a large midlatitude sink is in conflict with the data set of *Houghton* [1993a] [*Houghton*, 1993b].

We are not aware of global nitrogen fertilization estimates for earlier decades which consider all anthropogenic N sources. Thus we estimate in the following based on literature data upper bounds for past carbon storage by nitrogen fertilization. How much carbon has been sequestered by nitrogen fertilization depends (1) on how much of the anthropogenically fixed nitrogen has been deposited to the world's ecosystems, (2) how much of the deposited nitrogen has been converted to organic matter, and (3) in what proportion carbon and nitrogen has been built into organic matter.

1. *Peterson and Melillo* [1985] and *Schindler and Bayley* [1993] assumed in their estimates that only a small amount, that is, 6 and 13 TgN yr^{-1}, of the anthropogenically fixed nitrogen is available for nitrogen fertilization. On the other hand, *Galloway et al.* [1995] estimate that presently 80 TgN yr^{-1} out of 140 TgN yr^{-1} anthropogenically fixed carbon are reemitted to the atmosphere and that 60 TgN yr^{-1} is deposited again on continents either in the form of NH_x (40 TgN yr^{-1}) or as NO_3 (20 TgN yr^{-1}).

2. *Kinzig and Socolow* [1994] suggest that about 80 TgN yr^{-1} are presently taken up by living organisms or stored in the most labile part of the dead organic matter pool. *Schindler and Bayley* [1993] cite several

studies which indicate that around 90% of locally deposited nitrogen is retained in the investigated ecosystems. *Galloway et al.* [1995] remarks that enhanced denitrification on continents has the potential to be as large as 50-110 TgN yr^{-1}. However, no firm data on denitrification of anthropogenic nitrogen on land exist. A substantial amount of the deposited nitrogen (up to 40 TgN yr^{-1}) may be exported to coastal areas by riverine transport [*Galloway et al.*, 1995].

3. Carbon to nitrogen ratio in organic matter produced on land vary over more than 2 orders of magnitude [*Kinzig and Socolow*, 1994; *McGuire et al.*, 1992; *Peterson and Melillo*, 1985; *Schindler and Bayley*, 1993]. Soil C:N ratios vary between 4 and 50, whereas C:N ratios in vegetation are generally higher and can reach values up to 400 or more. *Peterson and Melillo* [1985] assume that about 90% of the nitrogen load is retained in soil compartments with a C:N ratio of about 10. *Schimel et al.* [1994] concludes that estimates of carbon storage higher than 1 GtC yr^{-1} are unrealistic because they assume that all of the N is stored in forms with high C:N ratios. On the other hand, *Schindler and Bayley* [1993] believe that the effective C:N ratio is in the range of 50-150. NH_4^+ seems to be stored mainly in soils, whereas a substantial portion of the deposited NO_3 is stored in aboveground vegetation. All of the nitrogen fixed by energy production is deposited in the form of NO_3, but only 20% of the nitrogen fixed by fertilizer and legume production is reemitted and deposited as NO_3 [*Galloway et al.*, 1995].

To estimate the potential of nitrogen fertilization, we accepted that 30% of N fixed by fertilizer and legume production is redistributed on land as NH_x, 5% as NO_3, and 100% of the N fixed by energy production is deposited as NO_3 [*Galloway et al.*, 1995, Figures 1 and 2]. We further assumed that the deposited NH_x (39 TgN yr^{-1}) is incorporated into organic material with a C:N ratio between 10 and 20 and deposited NO_3 (22 TgN yr^{-1}) with a ratio of 50-100. This yields a present potential for carbon storage of 1.5-3 GtC yr^{-1}. For 1960 emissions the maximum potential fertilization is then between 0.8 and 1.6 GtC yr^{-1}.

Anthropogenic nitrogen deposition in the open ocean may stimulate new production of order 0.1-0.2 GtC yr^{-1}. This is to small to have a significant impact on the atmospheric carbon inventory [*Joos et al.*, 1991]. Similarly, nitrogen input into coastal areas has probably a minor impact on atmospheric CO_2 [*Berner*, 1992].

To summarize, uncertainties in the link between the carbon and nitrogen cycle are very large. Under optimistic assumptions, nitrogen fertilization has the potential to support carbon storage of the order 1 GtC yr^{-1} during the last decades. However, it seems not likely that N fertilization alone stimulated a carbon storage of order 1 GtC yr^{-1} before 1960.

3.2.3. Climate variations. Different studies [*Houghton*, 1993a; *Dai and Fung*, 1993] suggested that climate variability may have contributed significantly to the carbon budget of the last decades. If climate variability has indeed a significant effect on terrestrial carbon storage, then atmospheric CO_2 must have varied in the past. In Figure 9, atmospheric CO_2 as reconstructed from several ice cores in Antarctica is plotted for the last millennium. The data vary between 272 and 287 ppm prior to the onset of the industrial revolution. A large part of this variation can be attributed to uncertainties in measurements and dating. Results of different ice cores are somewhat conflicting. *Siegenthaler et al.* [1988] and *Barnola et al.* [1995] suggested from their results (south pole and Adelie Land) that about 40 GtC of biospheric carbon were emitted to the atmosphere between 1200 and 1350. On the other hand, the Law Dome data (DE08 and DSS) do not show a significant CO_2 increase during that time. The ice core results suggest a decrease in atmospheric CO_2 of perhaps 4-8 ppm between 1550 and 1770. We have performed a deconvolution for the spline-fitted Law Dome data alone, thereby assuming that the observed CO_2 decrease is due to a terrestrial sink only. We found a cumulative sink of 30 GtC and a peak "biospheric" uptake of 1 GtC yr^{-1} between 1550 and 1620 . This suggests that it is not likely that climatic variations, such as little ice age type events, the medieval optimum, or the present warming, can stimulate a change in biospheric carbon inventory much larger than 40 GtC within 50 years.

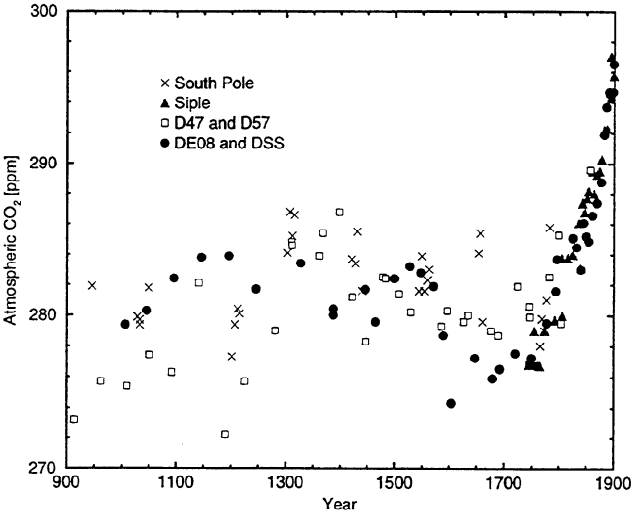

Figure 9. A reconstruction of the atmospheric CO_2 history for the last millennium as obtained by analyzing enclosed air bubbles in seven Antarctic ice cores [*Barnola et al.*, 1995; *Etheridge et al.*, 1996; *Neftel et al.*, 1985; *Siegenthaler et al.*, 1988]. Data scatter is due to both inaccuracies in individual measurements as well as to dating errors.

3.2.4. Combinations of factors. If we accept a conventional logarithmic relationship between primary productivity and atmospheric CO_2 then no single factor can explain the difference between nonfossil emissions and estimated land use data. Most likely, terrestrial carbon storage during the last decades was enhanced due to a combination of different mechanisms, like those mentioned above. Unfortunately, the above analysis is also hampered by the large uncertainties in the land use data (Table 2).

4. Summary and Conclusion

We have performed a deconvolution of high-precision ice core data from Law Dome site, Antarctica [*Etheridge et al.*, 1996]. The combined uncertainties of the deduced nonfossil emission term due to errors in CO_2 measurements, modeled ocean uptake, and fossil fuel data are estimated to be about 0.5 GtC yr^{-1} before 1950 and about 1 GtC yr^{-1} for the last decade. By applying a Monte Carlo technique we found a 2-σ uncertainty for the nonfossil emission (20 year average) to be 0.2-0.4 GtC yr^{-1} due to uncertainty in the ice core data. We interpreted the nonfossil emission term as a net biospheric sink or source. For the period 1800-1930 the deduced net biospheric source is around 0.5 GtC yr^{-1} in agreement with independent estimates of land use changes [*Houghton*, 1993a]. Thus the global carbon cycle appears to be balanced for this period.

We found a rapid change in the magnitude of the nonfossil term in the decade 1933-1943. After 1943, the deduced net biospheric uptake is around 0.3 GtC yr^{-1}. This implies an average biospheric sink of 1.5 GtC yr^{-1} during the last 5 decades to compensate carbon emissions by land use changes. We cannot easily attribute this sink to a single mechanism. The temporal pattern of this additional sink is not compatible with conventional estimates of carbon storage stimulated by elevated CO_2 levels. As an upper boundary, we estimated the potential terrestrial carbon storage induced by anthropogenic nitrogen loading to be around 1 GtC yr^{-1} for 1960 and between 1.5 and 3 GtC yr^{-1} at present time. It seems unlikely that anthropogenic nitrogen input into the world's ecosystems leads to carbon storage as large as 1 GtC yr^{-1} before 1960. Between 1935 and 1990 the cumulative biospheric sink is estimated to be 76 GtC. For comparison, we have analyzed observed CO_2 variability during the last millennium. Changes in biospheric carbon storage were found to be less than 40 GtC if assuming that the land biosphere alone is responsible for the observed CO_2 variations.

A proper understanding of the mechanism responsible for carbon storage on land is necessary to allow a credible estimate of the future magnitude of the terrestrial sink (or source). Our results suggest that the difference between the land use fluxes and the biospheric net uptake is probably due to a combination of factors. These may include climate variability, CO_2 and N fertilization, northern hemisphere forest regrowth, as well as uncertainties in the land use data and deconvolution analysis. While our study cannot explain the observed differences between land use data and nonfossil emissions, our results may serve as a constraint for future modeling studies of biospheric carbon storage. The study highlights also the need to better quantify historical land use emisssions including forest regrowth and the impact of changes in forest managment on atmospheric CO_2.

In this study we have interpreted the nonfossil emission to be of biospheric origin, thereby assuming that the natural carbon exchange between ocean and atmosphere is at balance on a decadal timescale. For the future we plan to include $\delta^{13}C$ data from the Law Dome site and atmospheric $\delta^{13}C$ data into our analysis. The isotopic signal will hopefully allow us to quantitatively disentangle the terrestrial and the oceanic carbon sink for the last 2 centuries using a different approach.

Acknowledgments. We thank D. Etheridge and coauthors for their generosity in providing us with their CO_2 data before publication. We highly appreciate that R. Francey and M. Leuenberger made their preliminary ^{13}C data available to us. We thank M. Heimann for discussion and for suggesting the Monte Carlo Analysis, R. Fink for providing his carbonate chemistry routines, and R. Marland for sharing his most recent fossil fuel emission data. We thank O. Marchal and N. Gruber for helpful comments. This work was funded by the U.S. Department of Energy (grant DE-FG02-90ER61054), the Swiss National Science Foundation, and the Electric Power Research Institute.

References

Andres, R. J., G. Marland, T. Boden, and S. Bischoff, Carbon dioxide emissions from fossil fuel combustion and cement manufacture 1751-1991 and an estimate of their isotopic composition and latitudinal distribution, in *The Carbon Cycle*, edited by T. M. L. Wigley and D. Schimel, Cambridge Univ. Press, New York, in press, 1996.

Barnola, J. M., M. Anklin, J. Procheron, D. Raynaud, J. Schwander, and B. Stauffer, CO_2 evolution during the last millennium as recored by Antarctic and Greenland ice, *Tellus, Ser. B, 47*, 264–272, 1995.

Bazzaz, F. A., The response of natural ecosystems to the rising global CO_2 levels, *Ann. Rev. of Ecol. Syst., 21*, 167–196, 1990.

Berner, R. A., Comments on the role of marine sediment burial as a repository for anthropogenic CO_2, *Global Biogeochem. Cycles, 6*(1), 1–2, 1992.

Chen, C.-T. A., The oceanic anthropogenic CO_2 sink, *Chemosphere, 27*(6), 1041–1064, 1993.

Ciais, P., P. P. Tans, M. Trolier, J. W. C. White, and R. J. Francey, A large northern hemispheric terrestrial CO_2 sink indicated by the $^{13}C/^{12}C$ ratio of atmospheric CO_2, *Science, 269*, 1098–1102, 1995.

Dai, A., and I. Y. Fung, Can climate variability contribute to the "missing" CO_2 sink, *Global Biogeochem. Cycles, 7*, 599–609, 1993.

D'Arrigo, R. D., and G. C. Jacoby, Tree-growth-climate relationships at the northern boreal forest tree line of North America: Evaluation of potential response to increasing carbon dioxide, *Global Biogeochem. Cycles*, 7(3), 525–535, 1993.

Dixon, R. K., S. Brown, R. A. Houghton, A. M. Solomon, M. C. Trexler, and J. Wisniewski, Carbon pools and flux of global forest ecosystems, *Science, 263*, 185–190, 1994.

Enting, I., C. Trudinger, and R. Francey, A synthesis inversion of the concentration and $\delta^{13}C$ of atmospheric CO_2, *Tellus, Ser. B, 47*, 35–52, 1995.

Enting, I. G., On the use of smoothing splines to filter CO_2 data, *J. Geophys. Res., 92*, 10977–10984, 1987.

Enting, I. G., T. M. L. Wigley, and M. Heimann, Future emissions and concentrations of carbon dioxide: Key ocean/atmosphere/land analyses, *technical report, Commonw. Sci. and Ind. Res. Org.*, Div. of Atm. Res., Melbourne, Victoria, Australia, *Tech. Rep.*, 1994.

Esser, G., Sensitivity of global carbon pools and fluxes to human and potential climatic impacts, *Tellus, Ser. B, 39*, 245–260, 1987.

Etheridge, D. M., L. P. Steele, R. L. Langenfelds, R. J. Francey, J.-M. Barnola, and V. I. Morgan, Natural and anthropogenic changes in atmospheric CO_2 over the last 1000 years from air in Antarctic ice and firn, *J. Geophys. Res., 101*, 4115–4128, 1996.

Francey, R. J., P. P. Tans, C. E. Allison, I. G. Enting, J. W. C. White, and M. Troller, Changes in oceanic and terrestrial carbon uptake since 1982, *Nature, 373*, 326–330, 1995.

Friedlingstein, P., I. Fung, E. Holland, J. John, G. Brasseur, D. Erickson, and D. Schimel, On the contribution of CO_2 fertilization to the missing biospheric sink, *Global Biogeochem. Cycles, 9*(4), 541–556, 1995.

Galloway, J. N., W. H. Schlesinger, H. Levy II, A. Michaels, and J. L. Schnoor, Nitrogen fixation: Anthropogenic enhancment-environmental response, *Global Biogeochem. Cycles, 9*(2), 235–252, 1995.

Gruber, N., J. L. Sarmiento, and T. F. Stocker, An improved method to detect anthropogenic CO_2 in the oceans, *Global Biogeochem. Cycles, 10*(4), 809–837, 1996.

Heimann, M., and C. D. Keeling, A three-dimensional model of atmospheric CO_2 transport based on observed winds, 2, Model description and simulated tracer experiments, in *Aspects of Climate Variability in the Pacific and the Western Americas, Geophys. Monogr. Ser., vol. 55*, edited by D. H. Peterson, pp. 237–275, AGU, Washington, D. C., 1989.

Heimann, M., and E. Maier-Reimer, On the relations between the oceanic uptake of CO_2 and its carbon isotopes, *Global Biogeochem. Cycles, 10*(1), 89–110, 1996.

Houghton, J. T., L. G. M. Filho, J. Bruce, H. Lee, B. A. Callander, E. Haites, N. Harris, and K. Maskell, *Climate Change 1994: Radiative Forcing of Climate Change and an evaluation of the IPCC IS92 Emission Scenarios. Report of Working Group I and III of the Intergovernmental Panel on Climate Change*, Cambridge Univ. Press,New York, 1994.

Houghton, J. T., L. G. M. Filho, B. A. Callander, N. Harris, A. Kattenberg, and K. Maskell, *Climate Change 1995-The Science of Climate Change: Contribution of WGI to the Second Assessment Report of the Intergovernmental Panel on Climate Change*, Cambridge Univ. Press, New York, 1996.

Houghton, R. A., Changes in terrestrial carbon over the last 135 years, in *The Global Carbon Cycle*, edited by M. Heimann, Volume I15, pp. 139–157, Springer-Verlag, 1993a.

Houghton, R. A., Is carbon accumulating in the northern temperate zone?, *Global Biogeochem. Cycles*, 7(3), 611–617, 1993b.

Inoue, H. Y., and Y. Sugimura, Variations and distributions of CO_2 in and over the equatorial Pacific during the period from the 1986/88 El Niño event to the 1988/89 La Niña event, *Tellus, Ser. B, 44*, 1–22, 1992.

Inoue, H. Y., and Y. Sugimura, Long-term trend of the partial pressure of carbon dioxide (pCO_2) in surface waters of the western North Pacific, 1984-1993, *Tellus, Ser. B, 47*, 391–413, 1995.

Joos, F., J. L. Sarmiento, and U. Siegenthaler, Estimates of the effect of Southern Ocean iron fertilization on atmospheric CO_2 concentrations, *Nature, 349*, 772–774, 1991.

Joos, F., M. Bruno, R. Fink, T. F. Stocker, U. Siegenthaler, C. Le Quéré, and J. L. Sarmiento, An efficient and accurate representation of complex oceanic and biospheric models of anthropogenic carbon uptake, *Tellus, Ser. B, 48*, 397–417, 1996.

Kauppi, P. E., K. Mielikainen, and K. Kuusela, Biomass and carbon budget of European forests, 1971 to 1990, *Science, 256*, 70–73, 1992.

Keeling, C. D., Industrial production of carbon dioxide from fossil fuels and limestone, *Tellus, 25*(2), 174–197, 1973.

Keeling, C. D., Global historical CO_2 emissions, in *Trends '93: A Compendium of Data on Global Change*, edited by T. Boden, D. Kaiser, R. Sepanski, and F. Stoss, pp. 501–504, Carbon Dioxide Inf. Anal. Cent., Oak Ridge, 1994.

Keeling, C. D., and T. P. Whorf, Atmospheric CO_2 records from sites in the SIO network, in *Trends '93: A Compendium of Data on Global Change*, edited by T. Boden, D. Kaiser, R. Sepanski, and F. Stoss, pp. 16–26, Carbon Dioxide Inf. Anal. Cent., Oak Ridge, 1994.

Keeling, C. D., R. B. Bacastow, A. F. Carter, S. C. Piper, T. P. Whorf, M. Heimann, W. G. Mook, and H. Roelofzen, A three-dimensional model of atmospheric CO_2 transport based on observed winds, 1., Analysis of observational data, in *Aspects of Climate Variability in the Pacific and the Western Americas, Geophys. Monogr. Ser., vol. 55*, edited by D. H. Peterson, pp. 165–237, AGU, Washington, D. C., 1989.

Keeling, C. D., T. P. Whorf, M. Wahlen, and J. v. d. Pflicht, Interannual extremes in the rate of atmospheric carbon dioxide since 1980, *Nature, 375*, 666–670, 1995.

Keeling, R. F., S. C. Piper, and M. Heimann, Global and hemispheric CO_2 sinks deduced from changes in atmospheric O_2 concentration, *Nature, 381*, 218–221, 1996.

King, A. W., W. R. Emanuel, S. D. Wullschleger, and W. M. Post, In search of the missing carbon sink: A model of terrestrial biospheric response to land-use change and atmospheric CO_2, *Tellus, Ser. B, 47*, 501–519, 1995.

Kinzig, A. P., and R. H. Socolow, Human impacts on the nitrogen cycle, *Phys. Today, 47*(11), 24–31, 1994.

Kolchugina, T. P., and T. S. Vinson, Carbon sources and sinks in forest biomes of the former Soviet Union, *Global Biogeochem. Cycles, 7*(2), 291–304, 1993.

Körner, C., CO_2 fertilization: The great uncertainty in future vegetation development, in *Vegetation Dynamics and Global Change*, edited by A. M. Solomon and H. H. Shugart, pp. 53–70, Chapman and Hall, New York, 1993.

Körner, C., and J. A. Arnone III, Responses to elevated carbon dioxide in artifical tropical ecosystems, *Science, 257*, 1672–1675, 1992.

Lüdeke, M. K. B., S. Dönges, R. D. Otto, J. Kindermann, F.-

W. Badeck, P. Ramge, U. Jäkel, and G. H. Kohlmaier, Response in NPP and carbon stores of the northern biomes to a CO_2-induced climatic change, as evaluated by the Frankfurt biosphere model (FBM), *Tellus, Ser. B, 47*, 191–205, 1995.

Marland, G., and R. M. Rotty, Carbon dioxide emissions from fossil fuels: A procedure for estimation and results for 1950-1982, *Tellus, Ser. B, 36*, 232–261, 1984.

Marland, G., T. A. Boden, and R. J. Andres. Global, regional and national annual CO_2 emission estimates from fossil-fuel burning, hydraulic-cement production and gas flaring: 1950 to 1992, *CDIAC Commun.*, Fall 1995.

McGuire, A. D., J. M. Melillo, L. A. Joyce, D. W. Kicklighter, A. L. Grace, B. Moore III, and C. J. Vorosmartyr, Interactions between carbon and nitrogen dynamcis in estimating net primary productivity for potential vegetation in North America, *Global Biogeochem. Cycles, 6*(2), 101–124, 1992.

Moore III, B., and B. H. Braswell, The lifetime of atmospheric carbon dioxide, *Global Biogeochem. Cycles, 8*(1), 23–38, 1994.

Neftel, A., E. Moor, H. Oeschger, and B. Stauffer, Evidence from polar ice cores for the increase in atmospheric CO_2 in the past two centuries, *Nature, 315*, 45–47, 1985.

Norby, R. J., C. A. Gunderson, S. D. Wullschleger, E. G. O'Neill, and M. K. McCracken, Productivity and compensatory response of yellow poplar trees in elevated CO_2, *Nature, 357*, 322–324, 1992.

Oechel, W. C., S. J. Hastings, G. Vourlitis, M. Jenkins, G. Riechers, and N. Grulke, Recent change of arctic tundra ecosystems from a net carbon dioxide sink to a source, *Nature, 361*, 520–523, 1993.

Oeschger, H., U. Siegenthaler, U. Schotterer, and A. Gugelmann, A box diffusion model to study the carbon dioxide exchange in nature, *Tellus, 27*, 168–192, 1975.

Peterson, B. U., and J. M. Melillo, The potential storage of carbon caused by eutrophication of the biosphere, *Tellus, 37*, 117–127, 1985.

Press, W. H., B. P. Flannery, S. A. Teukolsky, and W. T. Vetterling, *Numerical Recipes*, Cambridge Univ. Press, New York, 1989.

Quay, P. D., B. Tilbrook, and C. S. Wong, Oceanic uptake of fossil fuel CO_2: Carbon-13 evidence, *Science, 256*, 74–79, 1992.

Revelle, R., and H. E. Suess, Carbon dioxide exchange between atmosphere and ocean and the question of an increase of atmospheric CO_2 during the past decades, *Tellus, 9*, 18–27, 1957.

Sarmiento, J. L., and E. T. Sundquist, Revised budget for the oceanic uptake of anthropogenic carbon dioxide, *Nature, 356*, 589–593, 1992.

Sarmiento, J. L., J. C. Orr, and U. Siegenthaler, A perturbation simulation of CO_2 uptake in an ocean general circulation model, *J. Geophys. Res., 97*, 3621–3645, 1992.

Sarmiento, J. L., C. LeQuere, and S. W. Pacala, Limiting future atmospheric carbon dioxide, *Global Biogeochem. Cycles, 9*(1), 121–137, 1995.

Schimel, D., Terrestrial ecosystems and the global carbon cycle, *Global Change Biol., 1*(1), 77–91, 1995.

Schimel, D., I. Enting, M. Heimann, T. Wigley, D. Raynaud, D. Alves, and U. Siegenthaler, CO_2 and the carbon cycle, in *Climate Change 94, Radiative Forcing of Climate Change*, edited by J. Houghton, L. Meira-Filho, M. Bruce, H. Lee, B. Callander, E. Haites, N. Harris, and K. Maskell, pp. 38–71, Cambridge Univ. Press, New York, 1994.

Schimel, D., D. Alves, I. Enting, M. Heimann, F. Joos, D. Raynaud, and T. Wigley, CO_2 and the carbon cycle, in *IPCC Second Scientific Assessment of Climate Change*, edited by J. Houghton, pp. 76–86, Cambridge Univ. Press, New York, 1996.

Schindler, D. W., and S. E. Bayley, The biosphere as an increasing sink for atmospheric carbon: Estimates from increased nitrogen deposition, *Global Biogeochem. Cycles, 7*(4), 717–733, 1993.

Siegenthaler, U., El Niño and atmospheric CO_2, *Nature, 345*, 295–296, 1990.

Siegenthaler, U., H. Friedli, H. Loetscher, E. Moor, A. Neftel, H. Oeschger, and B. Stauffer, Stable-isotope ratios and concentration of CO_2 in air from polar ice cores, *Ann. Glaciol., 10*, 1–6, 1988.

Siegenthaler, U., and F. Joos, Use of a simple model for studying oceanic tracer distributions and the global carbon cycle, *Tellus, Ser. B, 44*, 186–207, 1992.

Siegenthaler, U., and H. Oeschger, Biospheric CO_2 emissions during the past 200 years reconstructed by deconvolution of ice core data, *Tellus, Ser. B, 39*(1-2), 140–154, 1987.

Siegenthaler, U., and J. L. Sarmiento, Atmospheric carbon dioxide and the ocean, *Nature, 365*, 119–125, 1993.

Stocker, T. F., W. S. Broecker, and D. G. Wright, Carbon uptake experiments with a zonally averaged global circulation model, *Tellus, Ser. B, 46*, 103–122, 1994.

Takahashi, T., T. T. Takahashi, and S. C. Sutherland, An assessment of the role of the North Atlantic as a CO_2 sink, *Philos. Trans. R. Soc. London, Ser. A, 348*(1324), 143–152, 1995.

Tans, P. P., J. A. Berry, and R. F. Keeling, Oceanic 12C/13C observations: A new window on ocean CO_2 uptake, *Global Biogeochem. Cycles, 7*(2), 353–368, 1993.

Tans, P. P., I. Y. Fung, and T. Takahashi, Observational constraints on the global atmospheric CO_2 budget, *Science, 247*, 1431–1438, 1990.

Toggweiler, J. R., K. Dixon, and K. Bryan, Simulations of radiocarbon in a coarse-resolution world ocean model. 1: Steady state prebomb distributions, *J. Geophys. Res., 94*, 8217–8242, 1989.

Townsend, A. R., B. H. Braswell, E. A. Holland, and J. E. Penner, Spatial and temporal patterns in terrestrial carbon storage due to the deposition of fossil fuel nitrogen, *Ecol. Appl., 6*(3), 806–814, 1996.

Volk, T., Effect of the equatorial Pacific upwelling on atmospheric CO_2 during the 1982-1983 El Nino, *Global Biogeochem. Cycles, 3*(3), 267–279, 1989.

Winguth, A. M. E., M. Heimann, K. D. Kurz, E. Maier-Reimer, U. Mikolajewicz, and J. Segschneider, El Niño-Southern Oscillation related fluctuations of the marine carbon cycle, *Global Biogeochem. Cycles, 8*(1), 39–63, 1994.

Wong, C. S., Y. H. Chan, and J. S. Pagey, Geographical, seasonal and interannual variations of air-sea CO_2 exchange in the subtropical Pacific surface waters during 1983-1988, 2, Air-sea CO_2 fluxes with skin-temperature adjustments, *Tellus, 47B*, 431–446, 1995.

M. Bruno and F. Joos, Physics Institute, University of Bern, Sidlerstr. 5, CH-3012 Bern, Switzerland. (e-mail: bruno@climate.unibe.ch; joos@climate.unibe.ch)

(Received July 10, 1996; revised November 6, 1996; accepted November 12, 1996.)